FINITE VOLUME CALCULATION OF TRANSONIC POTENTIAL FLOW THROUGH ROTORS AND FANS

by

Djordje S. Dulikravich*

and

David A. Caughey

FDA-80-03 March 1980

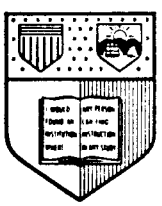

Fluid Dynamics and Aerodynamics Program

Sibley School of
Mechanical and Aerospace Engineering

Cornell University Ithaca, New York 14853

FINITE VOLUME CALCULATION OF TRANSONIC POTENTIAL FLOW THROUGH ROTORS AND FANS

by

Djordje S. Dulikravich*

and

David A. Caughey

FDA-80-03 March 1980

*Presently a National Research Council Research Associate at NASA Lewis Research Center, Computational Fluid Mechanics Branch, 5-9, Cleveland, Ohio 44135

FINITE VOLUME CALCULATION OF TRANSONIC POTENTIAL FLOW THROUGH ROTORS AND FANS

Djordje S. Dulikravich* and David A. Caughey

Sibley School of Mechanical and Aerospace Engineering
Cornell University, Ithaca, N.Y.

ABSTRACT

An analysis was carried out for steady, transonic, potential, lifting flows through two dimensional stationary airfoil cascades and three dimensional, rotating cascades mounted on doubly infinite cylindrical hubs. The exact full potential equation was derived in its canonical form with appropriate boundary and periodicity conditions for these cases.

Two separate computer programs were developed which numerically solve that equation, allowing for arbitrary airfoil shapes and blade taper, sweep, dihedral and twist distributions as well as for the occurrence of weak shocks. The computational domain was formed using a sequence of geometric transformations of the physical domain resulting in a boundary fitted coordinate system.

A locally type dependent rotated finite difference scheme was coupled with a successive line over-relaxation technique to iteratively solve the artificially time dependent generalized form of the full potential equation. The artificial viscosity required for this shock capturing technique was added in conservation form, while residues were defined using a non-conservative isoparametric linear finite volume technique.

These algorithms can serve for the flow prediction about stream deflectors, isolated propellers, hovering rotors, wind turbines, ducted fans, stators and finned missiles.

*Presently a National Research Council Research Associate at NASA Lewis Research Center, Computational Fluid Mechanics Branch, 5-9, Cleveland, Ohio 44135

Introduction

The problem to be solved can be formulated in two stages. The first is the mathematical modelling of the physical phenomena that occur in the gas flow through rotating turbomachinery passages and through planar cascades of airfoils representing aerodynamic deflectors or nozzles.

The second part is the development of computer programs implementing the appropriate numerical techniques that will perform the solution procedures of these analytical models. The main objective of this work is to devise algorithms that will require minimum computation time and storage. It is also desirable to solve a broad class of similar problems with only minor changes in the input data, and to provide a basis for the development of new computer programs that will solve even more complicated mathematical models and be applicable to more general configurations.

As summarized in the paper of Foley (1976), the analytical models that were developed prior to about 1950 were very simple and approximate. The main disadvantage of all these theories was the assumption that the fluid is incompressible. The effect of compressibility, the shape and relative size of the hub and the blade tip, and most importantly the features of the rotating cascade flow, were accounted for by the use of empiricism.

The most recent period is one that started with the basic paper of Wu (1952) in which he developed the exact Full Potential Equation (FPE) for an homentropic, inviscid, nonconducting, nonradiating compressible fluid flowing with zero absolute vorticity through rotating cascades.

The FPE is a quasiliniear partial differential equation of mixed type and because of this nonlinearity it can exhibit weak solutions (Carrier and Pearson, 1976) containing mathematical discontinuities in the solution or its derivatives. These weak solutions are acceptable when the FPE is expressed in conservation form, because through such isentropic discontinuities the mass,

entropy and energy are conserved, while linear momentum is not conserved in the direction normal to such a discontinuity (Steger and Baldwin, 1972; Caughey, 1978).

The major drawback of the FPE model of the actual physical process is that it neglects entropy variations. This means that it does not incorporate the second law of thermodynamics and as a consequence admits both compression and expansion discontinuities as valid parts of the solution. It is therefore important to distinguish between such isentropic shocks and the Rankine-Hugoniot shocks which have the property of not conserving the entropy and in such a way discarding the physically unrealizable expansion shocks.

Because of the need for high accuracy in the application of the boundary conditions in the case of transonic internal flows, as well as the complexity of the Small Perturbation Equation (SPE) approximation to the FPE (as shown by Rae, 1976), the exact FPE was solved using a boundary fitted coordinate system in order to apply boundary conditions without approximations.

II. Boundary Conforming Mesh

Finite difference solutions are most easily and efficiently carried out in rectangular computational domains that are also boundary-conforming (or body-fitted). Also, in order to avoid stability problems and to maximize the convergence rate of the iterative solution, one should try to distribute the mesh cells in a smoothly varying fashion, while at the same time trying to cover parts of the flow field where flow parameters exhibit higher gradients with a finer mesh.

These requirements can be most nearly met (at least in two-dimensional surfaces) by the use of a conformal mapping of the physical flow region (x,y) onto a rectangular computational domain (X,Y). In such a problem one is faced with the unpleasant task of numerical evaluation of elliptic integrals and other

higher order transcendental functions (Ives and Liutermoza, 1976) which is time consuming, still not exact and often unstable.

In our case the physical space has been transformed into a computational X,Y,Z space which does not have to be precisely orthogonal. This implies that we do not have to map the actual flow domain conformally. Consequently, one can think of a cascade of airfoils as being approximated by a cascade of slits of zero thickness. An analytic function was chosen of the form

$$\tilde{w} = e^{i\beta} \ell n \frac{m-\tilde{z}}{m+\tilde{z}} + e^{-i\beta} \ell n \frac{1-m\tilde{z}}{1+m\tilde{z}}$$

which is shown (Kober, 1957) to map conformally a cascade of unit circles (each on a different Riemann sheet in the $\tilde{z} = x + iy$ plane) with a slit in the middle whose endpoints are situated at $\tilde{z} = \pm m$ (see Fig. 1) onto a cascade of slits in the $\tilde{w} = x + iy$ plane and spaced $2\pi\cos\beta$ distance apart, where β is the stagger angle of the cascade. This analytic function is unfortunately not analytically invertible except in the case of zero stagger (Garrick, 1944). Therefore it was inverted iteratively using a simple Newton-Raphson method.

From the $\tilde{z}$-plane to the $\tilde{Z}$-plane there is one additional step, effected by the introduction of elliptic polar coordinates (u_e, v_e)

$$\xi = m \cosh u_e \cos v_e$$
$$\eta = m \sinh u_e \sin v_e$$

One family of these coordinates (u_e = const.) is a system of ellipses that vary in eccentricity from a slit to a circle at large distances (Spiegel, 1968). Hence they nearly conform with the slit-circle z-plane. The other family of

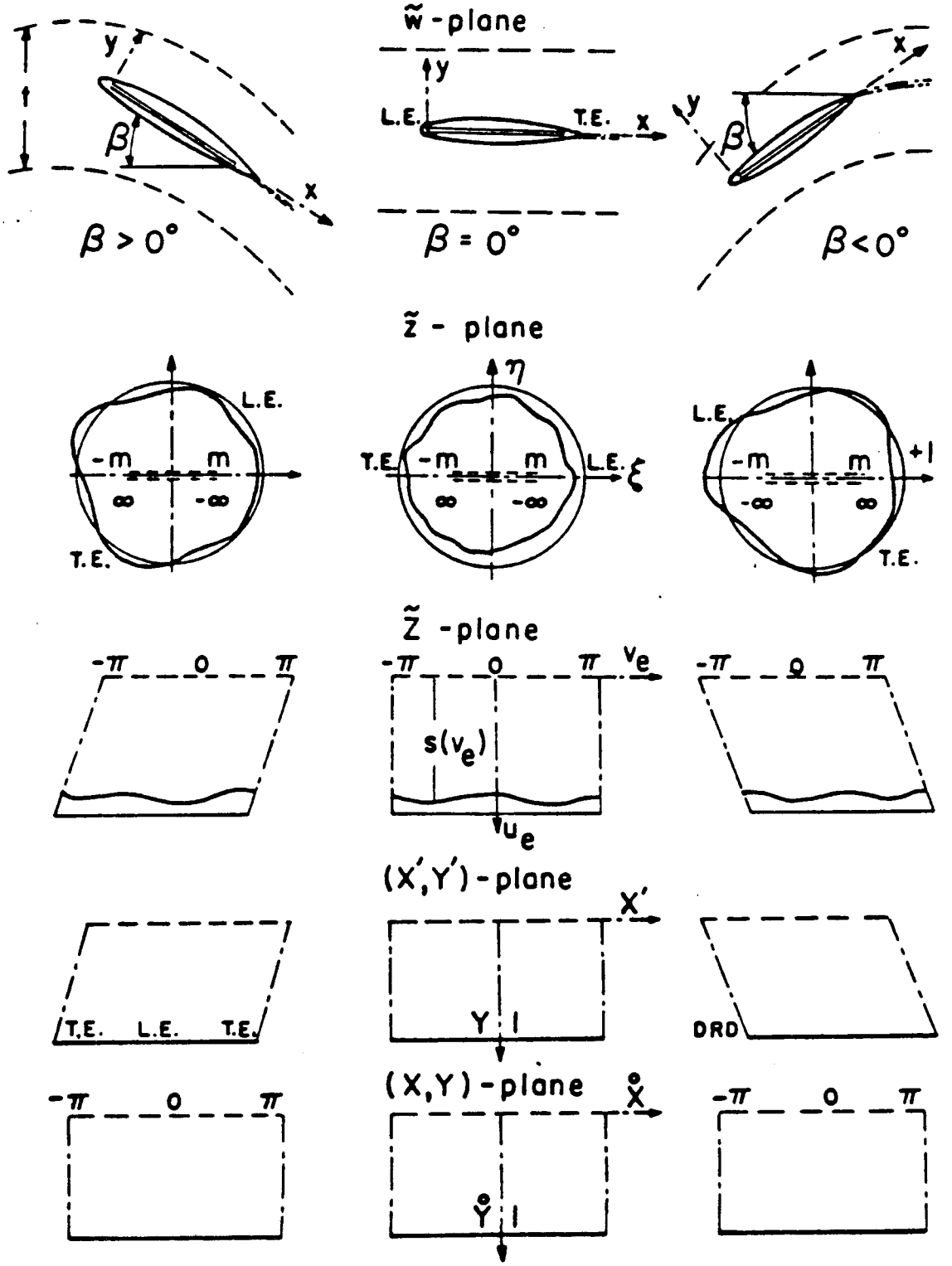

Fig. 1. Geometric Transformation Sequence

coordinates (v_e = const.) is a family of hyperbolas orthogonal to the first coordinate family of ellipses. The domain outside of an actual airfoil will map onto a nearly circular domain in the z-plane, instead of onto an exact circle as in the case of the zero thickness slit. The subsequent introduction of elliptic coordinates will not help to eliminate this problem entirely and one side of the computational domain will be an irregular line. In order to make it as smooth as possible, (thus ensuring at least locally the condition of equal curvature of the profile and the enveloping family of elliptic mesh lines) Theodorsen (1931) has shown that the endpoints of the slit should be positioned approximately midway between the edges and their centers of curvature.

The easiest way to convert this shape into the desired rectangular shape is by use of the shearing transformation (see Fig. 1):

$$X' = v_e \quad ; \quad -\pi + DRD \leq X' \leq \pi + DRD$$

$$Y' = \frac{u_e}{s(v_e)} \quad ; \quad 0 \leq Y' \leq +1$$

The requirement of mesh orthogonality in the physical space is not absolutely necessary in our method as it is in the methods of other researchers using conformal transformations (Ives and Liutermoza, 1976). Therefore, the present method is more promising for completely arbitrary 2-D and especially 3-D configurations.

The basic idea of separately transforming each distorted mesh cell (Fig. 2) from the (x,y,z) space into a computational (X,Y,Z) cube by use of the linear Lagrangian interpolation polynomials in the closed interval (-1,+1) has been only recently applied in finite difference methods in aerodynamics. It is called the "finite volume technique" (Jameson and Caughey, 1977; Caughey and

Jameson, 1977). It combines the simplicity of finite differencing with the geometrical versatility of the finite element technique.

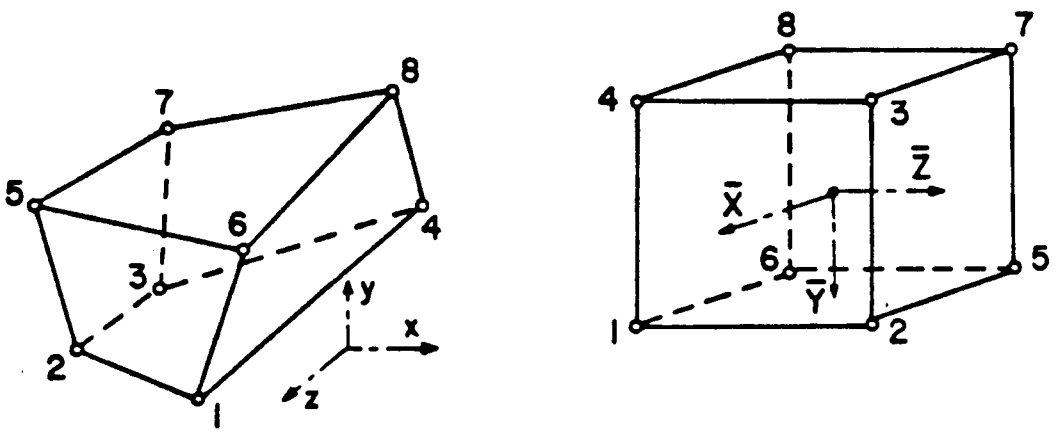

Fig. 2. Trilinear Finite Volume Transformation

The trilinear function that separately maps each elementary distorted parallelepiped from discretized (x,y,z) physical space into a separate cube of sides $\Delta X = \Delta Y = \Delta Z = 2$in the discretized computational space (X,Y,Z) can be written in the following form.

Let each corner of the 3-D element be designated by a different value of p where $p = 1,2,\ldots,8$, and $\bar{X},\bar{Y},\bar{Z}$ be local coordinates within each cell, i.e., (see Fig. 2)

$$\bar{X}_p = \pm 1 \qquad \bar{Y}_p = \pm 1 \qquad \bar{Z}_p = \pm 1 \ .$$

Then with the isoparametricity assumption (that geometric and flow properties are mapped within each Elementary Mesh Cell (EMC) by the same function) if b stands for any of the following: x,y,z,G(x,y,z) or $\phi(x,y,z)$, we can write

$$b = \frac{1}{8} \sum_{p=1}^{8} b_p (1+\bar{X}_p \bar{X})(1+\bar{Y}_p \bar{Y})(1+\bar{Z}_p \bar{Z}) \ .$$

The linear nature of these functions constrains the edges connecting the corner points of an EMC to be straight lines in the physical space. This represents a simplification in the discretized treatment of the actual shape of solid surfaces and requires higher EMC concentration in regions where the boundaries have high curvature.

III. Mathematical Model in the (x,y,z) Space

The relative coordinate system (x,y,z) is fixed for a blade. The free-stream is rotating at the constant angular speed $|\vec{\Omega}|$ about the axis of rotation x and advancing along the same axis at the constant speed U_∞ (Fig. 3).

The relative velocity $\vec{V}_r$ of fluid with respect to the propeller is:

$$\vec{V}_r = q_r \hat{e}_s = u_r \hat{e}_x + v_r \hat{e}_y + w_r \hat{e}_z$$

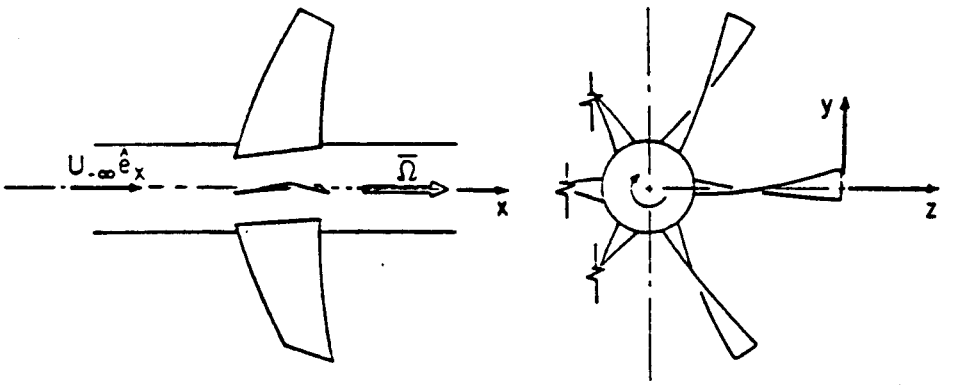

Fig. 3. The Physical (x,y,z) Space.

Then the absolute fluid velocity $\vec{V}$ is the sum of the relative velocity $\vec{V}_r$ and the rotational transfer velocity $(\vec{\Omega} \times \vec{r})$.

$$\vec{V} = \vec{V}_r + (\vec{\Omega} \times \vec{r}) = u\hat{e}_x + v\hat{e}_y + w\hat{e}_z$$

where $\vec{r} = (y^2 + z^2)^{1/2}\hat{e}_r$ is a position vector in the (y,z) rotor plane.

In the absence of body forces, the equation for the conservation of linear momentum in the case of the steady rotating flow of a compressible inviscid fluid expressed in the relative coordinate system is:

$$(\vec{V}_r \cdot \vec{\nabla})\vec{V}_r - \Omega^2\vec{r} + 2(\vec{\Omega} \times \vec{V}_r) = -\frac{1}{\rho}\vec{\nabla} p$$

where p is static pressure and ρ is fluid density. With the additional assumption that the fluid is homocompositional and that it was initially absolutely irrotational i.e., that

$$\vec{\nabla} \times \vec{V} = 0$$

it can be shown (Wu, 1952) that it will remain absolutely irrotational throughout the flowfield (according to Kelvin's Theorem) only if the conditions of the homentropic character of the flow

$$\vec{\nabla}S = 0$$

and the condition of the uniform rothalpy I (Vavra, 1960)

$$\vec{\nabla}I = \vec{\nabla}h + \frac{1}{2}\vec{\nabla}(\vec{v}_r \cdot \vec{v}_r - \Omega^2 r^2) = 0$$

where h is static enthalpy, are satisfied simultaneously everywhere in the flowfield.

Under these assumptions we are able to introduce the absolute velocity potential ϕ defined as

$$\vec{v} = \vec{\nabla}\phi$$

consequently decreasing the number of variables involved in the analytical formulation of the problem and improving the simplicity and speed of the computations.

The continuity equation for the rotating, steady flow is then:

$$a^2\vec{\nabla} \cdot \vec{v}_r - (\vec{v}_r \cdot \vec{\nabla})Q = 0$$

where

$$Q = \frac{1}{2}(q_r^2 - \Omega^2 r^2)$$

$$q_r = |\vec{v}_r| = |u_r\hat{e}_x + v_r\hat{e}_y + w_r\hat{e}_z|$$

Its scalar form expressed in (x,y,z) physical space and written in a quasi-linear form (Dulikravich, 1979) is then:

$$a^2(u_{r,x}+v_{r,y}+w_{r,z}) - (u_r Q_{,x}+v_r Q_{,y}+w_r Q_{,z}) = 0 \qquad (1)$$

where the local speed of sound is:

$$a^2 = a^2_{-\infty} + \frac{(K-1)}{2}(2Q_{-\infty}-2Q)$$

where $K = C_p/C_v$ is the ratio of the specific heats.

III-a. Boundary Conditions

Assuming that each fluid particle at upstream infinity has the same total energy in the non-rotating frame (equivalent to total enthalpy in adiabatic processes)

$$H_{-\infty} = h_{-\infty} + \frac{V^2_{-\infty}}{2} = \text{const.}$$

and uniform rothalpy

$$I = H - (\vec{\Omega} \times \vec{r}) \cdot \vec{V} = \text{const.}$$

it follows that

$$H_{-\infty} - I_{-\infty} = (\vec{\nabla}\phi)_{-\infty} \cdot (\vec{\Omega} \times \vec{r})_{-\infty} = \vec{V}_{-\infty} \cdot (\Omega r)\hat{e}_\theta = \text{const.}$$

It is easy to check that only flows with absolute velocity at upstream infinity equal to

$$\vec{V}_{-\infty} = (\vec{\nabla}\phi)_{-\infty} = U_{-\infty}\hat{e}_x + \frac{C_\theta}{r}\hat{e}_\theta$$

(where $U_{-\infty}$ and C_θ are constants) simultaneously satisfy this irrotationality condition and the continuity equation.

Therefore the absolute flow at upstream infinity in the general case can be generated by the superposition of a uniform stream in axial direction and a 2-D potential vortex (generated, say, by an upstream stator) in the plane perpendicular to the axial stream.

On the surface of the blade or hub the boundary condition is

$$\vec{V}_r \cdot \vec{\nabla}F = 0$$

where $F(x,y,z) = 0$ is the equation of the solid surface. In the case of a ducted or shrouded propeller, boundary condition on the surface of a shroud is

$$\vec{\nabla}\phi \cdot \vec{\nabla}F = 0 \ .$$

In the study of two-dimensional flows, a branch cut of arbitrary shape must be inserted in the flow field to render solutions with non-zero circulation single-valued when using the velocity potential. This cut is conveniently assumed to leave the trailing edge. The finite discontinuity in the velocity potential at the trailing edge is equal to the circulation Γ of the velocity

field. This constant discontinuity (i.e., no-jump in static pressure) is preserved at every point of the cut all the way to downstream infinity.

In the case of three-dimensional flow, the difficulties associated with the iterative determination of the convection and roll-up of the trailing vortex sheet are avoided by applying a linearized condition on a surface whose position is determined a priori. Note that such an arbitrarily prescribed shape of the vortex sheet will violate the kinematic condition at the sheet (Kaiho, 1978; Robinson and Laurman, 1965), i.e., the shape will not in general be a stream surface and, therefore, it will not be a true contact discontinuity (Hayes, 1960).

The dynamic condition that the static pressure is continuous through the vortex sheet is approximately preserved by enforcing the jump in the potential at every point of the intersection of the vortex sheet and a cylindrical cutting surface r = const. to be equal to the difference in the potential at the corresponding trailing edge point.

The condition that the velocity vector is a periodic function must be applied along the identically shaped and periodically positioned boundaries.

The reduced velocity potential G is introduced for the two-dimensional case according to

$$\phi(x,y) = U_{\infty}(x\cos\alpha_{\infty}+y\sin\alpha_{\infty}) + G(x,y) + \text{const.}$$

where α_{∞} is the free stream angle at upstream infinity. A similar definition is used in the 3-D case:

$$\phi(x,r,\theta) = (U_{\infty}x + C_{\theta}\theta) + G(x,r,\theta) + \text{const.}$$

Then the periodicity condition can be actually applied in terms of the reduced potential G. In the two-dimensional case it is

$$G(x,y) = G(x,y+h)$$

and in the three-dimensional case

$$G(x,r,\theta) = G(x,r,\theta+2\pi/B)$$

where B is the number of blades.

The boundary conditions at upsteam and radial infinities are:

$$G(x_{-\infty},r,\theta) = G(x,r_{+\infty},\theta) = 0$$

If the density and velocity are normalized by their values at upstream infinity, mass conservation in two-dimensional case requires

$$\cos\alpha_{-\infty} = \rho_{+\infty}\, q_{+\infty}\, \cos\alpha_{+\infty} ,$$

and one can iteratively determine $q_{+\infty}$ and set the boundary conditions at the downstream infinity to be:

$$(G_{,x})_{+\infty} = q_{+\infty}\cos\alpha_{+\infty} - \cos\alpha_{-\infty}$$

Values of $M_{-\infty}$, $\alpha_{-\infty}$ and $\alpha_{+\infty}$ must be specified for a two-dimensional case.

Following the derivations of Okurounmu and McCune (1970) it can be shown from the condition of zero mass flow perturbation at downstream infinity, that

the corresponding linearized boundary condition in the three-dimensional case is

$$(G_{,x})_{+\infty} = \frac{B\Omega}{\pi(1-M_{-\infty}^2)(\eta_t^2-1)(q_r^t)_{-\infty}} \int_1^{\eta_{+\infty}} \Gamma(\eta)\eta \, d\eta - \frac{B\Omega}{2\pi(q_r^t)_{-\infty}} \Gamma(r)$$

where:
$$M_{-\infty} = U_{-\infty}/a_{-\infty}$$
$$\eta_t = r_{tip}/r_{hub}$$
$$\eta_{+\infty} = r_{+\infty}/r_{hub}$$
$$q_r^t = |\vec{V}_r|_{tip}$$

III.2. Relative Streamline Aligned Space

The answer to the problem of nonuniqueness of the solution of FPE is the provision of the proper domain of influence of the partial differential equation at every mesh point. In the case when the FPE is locally elliptic (i.e., the flow is subsonic at the point) all surrounding points influence the value of a variable at the point in question. Therefore, central difference formulas should be used at such a point. The correct domain of influence of the locally hyperbolic FPE can be found by using the method outlined by Von Mises (1958). It consists of writing momentum, mass and energy conservation equations in an orthogonal coordinate system (s,n,m) aligned locally with the relative velocity vector $\vec{V}_r$ where s is relative streamline coordinate and n and m are mutually orthogonal directions forming a plane locally perpendicular to the relative streamlines. In three dimensions the domain of dependence is a conoid having the relative streamline as a centerline and opening up in the upstream direction.

Therefore at supersonic points one should perform strictly upwind differencing for the streamwise differences in order to most closely approximate the

local shape and effect of the analytical domain of influence of the locally hyperbolic FPE. This means that only these second derivatives of ϕ in the (X,Y,Z) computational space that form the term $\phi_{,ss}$ will be backward or upstream differenced in the case of locally supersonic relative flow. By doing so, we introduce a truncation error into the numerical evaluation of the $\phi_{,ss}$ term, which is proportional to $\phi_{,sss}$ and can be thought of as an artificial dissipative or viscous term. It is important to stress the fact that we are numerically solving a nondissipative FPE. Because the physical (molecular) viscosity is postulated to be equal to zero, the artificial viscosity that has been numerically introduced has no physical counterpart. It is more obvious if one notices that the term, $\phi_{,sss}$ is of the order of the mesh size (Jameson, 1976) and as the mesh size goes to zero, the value of the artificial viscosity term (if introduced in conservation form) will vanish, giving in the limit an exact solution to the actual FPE without dissipation.

The FPE for three-dimensional, rotating, steady flows can be written (Dulikravich, 1979) in its exact operator canonical form as:

$$[(a^2-q_r^2)(\phi^H_{,ss}-\phi^E_{,ss})+(a^2\nabla^2\phi^E-q_r^2\phi^E_{,ss})] = 0 \qquad (2)$$

where all the second derivatives of ϕ with respect to X,Y,Z coordinates that are designated by the superscipt H are approximated by retarded or backward differences, while those designated by the superscript E are approximated by central differences. Note that when $\Omega = 0$ (i.e., when $\vec{V}_r = \vec{V}$ and consequently $q_r = q$) one recovers the canonical form of the FPE for the nonrotating steady flow obtained by Jameson (1974):

$$[(a^2-q^2)\phi^H_{,ss}+a^2(\nabla^2\phi^E-\phi^E_{,ss})] = 0$$

IV. Mathematical Model in Computational Domain

The FPE must be transformed further into the (X,Y,Z) computational space for the purpose of the type-dependent finite-difference evaluation of its second derivatives and consequent determination of the coefficient matrix for the relaxation process. Let [J] represent the geometric transformation matrix

$$[J] = \begin{bmatrix} x_{,X} & x_{,Y} & x_{,Z} \\ y_{,X} & y_{,Y} & y_{,Z} \\ z_{,X} & z_{,Y} & z_{,Z} \end{bmatrix}$$

Then

$$\{\nabla_{XYZ}\} = [J^T]\{\nabla_{xyz}\} \therefore [\nabla_{xyz}] = [\nabla_{XYZ}][J^{-1}]$$

where $\{\nabla_{XYZ}\}$ is a column vector form of a linear vector operator in (X,Y,Z) space, while $\{\nabla_{xyz}\}$ is a column vector of the same operator in the physical (x,y,z) space. The determinant of [J] will be designated by D. Also, let B_{ij} be the elements of the symmetric matrix

$$[B] = [J^T J]^{-1} = [J^{-1}][J^T]^{-1} .$$

We further define the modified contravariant components of the relative velocity vector in the (X,Y,Z) space as:

$$\begin{Bmatrix} U_r \\ V_r \\ W_r \end{Bmatrix} = D[J^{-1}] \begin{Bmatrix} u_r \\ v_r \\ w_r \end{Bmatrix} = D[J]^{-1} \begin{Bmatrix} 0 \\ \Omega z \\ -\Omega y \end{Bmatrix} + D[B] \begin{Bmatrix} \phi_{,X} \\ \phi_{,Y} \\ \phi_{,Z} \end{Bmatrix} \qquad (3)$$

Then

$$\phi_{,ss} = \frac{1}{D^2 q_r^2}\left(U_r^2\phi_{,XX}+V_r^2\phi_{,YY}+W_r^2\phi_{,ZZ}+2U_rV_r\phi_{,XY}+\right.$$

$$\left.+2U_rW_r\phi_{,XZ}+2V_rW_r\phi_{,YZ}\right)+$$

$$+\left(\begin{array}{l}\text{terms not including}\\ \text{second derivatives of }\phi\end{array}\right) \qquad (3)$$

Also

$$\nabla^2_{XYZ} = [\nabla_{XYZ}][B]\{\nabla_{XYZ}\} = B_{11}\phi_{,XX}+B_{22}\phi_{,YY}+B_{33}\phi_{,ZZ}+2B_{12}\phi_{,XY}+$$

$$+2B_{13}\phi_{,XZ}+2B_{23}\phi_{,YZ}+\left(\begin{array}{l}\text{terms not including}\\ \text{second derivatives of }\phi\end{array}\right) \qquad (4)$$

Then, after premultiplying Eq. (2) by D and expressing the appropriate variables in terms of the second derivatives of ϕ and collecting like terms, one arrives at the modified FPE:

$$S_{XX}\phi^E_{,XX}+S_{YY}\phi^E_{,YY}+S_{ZZ}\phi^E_{,ZZ}+S_{XY}\phi^E_{,XY}+S_{XZ}\phi^E_{,XZ}+$$

$$+S_{YZ}\phi^E_{,YZ}+R_{XX}(\phi^H_{,XX}-\phi^E_{,XX})+R_{YY}(\phi^H_{,YY}-\phi^E_{,YY})+$$

$$+R_{ZZ}(\phi^H_{,ZZ}-\phi^E_{,ZZ})+R_{XY}(\phi^H_{,XY}-\phi^E_{,XY})+$$

$$+R_{XZ}(\phi^H_{,XZ}-\phi^E_{,XZ})+R_Y(\phi^H_{,YZ}-\phi^E_{,YZ})+$$

$$+\left(\begin{array}{l}\text{terms not including}\\ \text{second derivatives of }\phi\end{array}\right)=0 \qquad (5)$$

This form will be used for the finite volume evaluation of the matrix $[\delta]$ of the correction coefficients to the potential .

The coefficients in the above equation can be determined from Eq. (3) and Eq. (4) to be:

$$\mu = \max\{(1-a^2/q_r^2);\ 0.\}$$

$$S_{XX} = a^2 DB_{11} - U_r^2/D$$

$$S_{YY} = a^2 DB_{22} - V_r^2/D$$

$$S_{ZZ} = a^2 DB_{33} - W_r^2/D$$

$$S_{XY} = 2(a^2 DB_{12} - U_r V_r/D)$$

$$S_{XZ} = 2(a^2 DB_{13} - U_r W_r/D)$$

$$S_{YZ} = 2(a^2 DB_{23} - V_r W_r/D)$$

$$R_{XX} = -\mu U_r^2/D$$

$$R_{YY} = -\mu V_r^2/D$$

$$R_{ZZ} = -\mu W_r^2/D$$

$$R_{XY} = -2\mu U_r V_r/D$$

$$R_{XZ} = -2\mu U_r W_r/D$$

$$R_{YZ} = -2\mu V_r W_r/D$$

The conservation form of the continuity equation

$$\vec{\nabla} \cdot (\rho \vec{V}_r) = \frac{1}{D}\left((\rho U_r)_{,x} + (\rho V_r)_{,y} + (\rho W_r)_{,z}\right) = 0$$

that was (in the case of non-rotating flows) used originally by Jameson (Jameson and Caughey, 1977) for the finite volume evaluation of the residuals of the FPE in conservation form, involved the time consuming evaluation of the local fluid density. In order to avoid this,

Caughey (Caughey and Jameson, 1977) wrote the continuity equation in a nondivergence (nonconservative) form similar to Eq. (1). After premultiplication by Da^2/ρ, Eq. (1) then transforms (Dulikravich, 1979) into:

$$a^2(U_{r,X}+V_{r,Y}+W_{r,Z}) - (U_rQ_{,X}+V_rQ_{,Y}+W_rQ_{,Z}) = 0 \qquad (7)$$

Eq. (7) will be used exclusively for the finite volume calculation of the residuals of the discretized form of the transformed continuity equation.

IV.2. Boundary Conditions

The blade surface (F = Y-const.) boundary condition becomes: $V_r = 0$, while the hub surface (F = Z-const.) boundary condition becomes: $W_r = 0$. In the case of a ducted fan, the boundary condition on the inner surface of the shroud is:

$$W_r = \Omega((z_{,X}x_{,Y}-x_{,X}z_{,Y})z - (x_{,X}y_{,Y}-y_{,X}x_{,Y})y)$$

which in the case of a cylindrical shroud as well as in the nonrotating case

becomes: $W_r = 0$. Boundary conditions at upstream and radial infinities (in the case of an isolated propeller) do not change during the transformation nor do the jump conditions on the 2-D cut and 3-D vortex sheet.

The periodicity conditions in the 2-D computational space (see Fig. 1) are:

$$G(X+b,o) = G(X-b,o)$$

and in 3-D case:

$$G(X+b,o,Z) = G(X-b,o,Z)$$

where

$$b \leq \pi \ .$$

V. Numerical Solution

V.1. Artificial Time Concept

Because the FPE cannot be solved analytically for the cases studied, it was discretized and solved numerically using a Successive Line Over Relaxation (SLOR) algorithm.

The 3-D steady state FPE that we wish to solve can be written (see Eq. (2) in the following form:

$$(M_r^2-1)\phi_{,ss}-\phi_{,mm}-\phi_{,nn} = \left(\begin{array}{l}\text{terms not explicitly involving}\\ \text{second derivatives of } \phi\end{array}\right)$$

One can consider this to be the steady state limit of the more general (Garabedian, 1956; Jameson, 1974) Artificial Time-Dependent Equation (ATDE)

$$(M_r^2-1)\phi_{,ss}-\phi_{,mm}-\phi_{,nn}+2\alpha_1\phi_{,st}+2\alpha_2\phi_{,mt} +$$

$$+ 2\alpha_3\phi_{,nt}+\varepsilon\phi_{,t} = R^* \qquad (8)$$

where ε is a damping coefficient and R^* represents a group of terms involving neither second spatial derivatives of ϕ nor artificial time derivatives. By using the transformation (Jameson, 1974)

$$T = t + \frac{\alpha_1 s}{M_r^2-1} - \alpha_2 m - \alpha_3 n$$

the ATDE acquires a new form which is easier to analyse

$$(M_r^2-1)\phi_{,ss}-\phi_{,mm}-\phi_{,nn}-\{\frac{\alpha_1^2}{M_r^2-1}-\alpha_2^2-\alpha_3^2\}\phi_{,TT}+\epsilon\phi_{,T}=R^*$$

When $M_r < 1$ the artificial time is a time-like direction and therefore the spatial sweeping direction is completely arbitrary. When the relative flow is locally supersonic, $M_r > 1$. The solution of the locally hyperbolic FPE (which is a steady state equation) must correspond to the steady state solution of the ATDE Eq. (8) for large values of the artificial time. This means that the s direction (the relative streamline direction) must be the time-like (or sweeping) direction of the unsteady problem if one wants to avoid the problem of ultra-hyperbolicity. The requirement that

$$\alpha_1^2 > (M_r^2-1)(\alpha_2^2+\alpha_3^2) \tag{9}$$

must be satisfied when $M_r > 1$, i.e., that the α_1 term in Eq. (8) must always have a non-zero value. When $M_r \doteq 1$ this condition can be secured by the addition of an explicit $\phi_{,st}$ term to the Eq. (8) as explained by Jameson (1974). In the present work, artificially time dependent differencing was used in the way suggested by Jameson (1974), who considered iteration sweeps through the computational field as successive intervals in an artificial time.

Designating with superscript "+" the new value of the variable (i.e., one that will be obtained as the result of the current iteration sweep through the field), with no superscript designating the temporary value of the variable on a particular column during the iteration sweep, and with the superscript "o" designating all old values (obtained after the previous iteration sweep), one can write the new velocity potential ϕ^+ at the particular mesh point (i,j,k) as

$$\phi^+_{i,j,k} = \phi^o_{i,j,k} - C_{i,j,k} \tag{10}$$

where $C_{i,j,k}$ is the correction to be subtracted from the potential at the point (i,j,k) during the present iteration sweep. The use of the SLOR technique requires introduction of a temporary or provisional value of the potential ϕ at every mesh point on the line along which SLOR is to be applied. The definition of such a term is

$$\phi_{i,j,k} = \frac{1}{\omega}\,\phi^{+}_{i,j,k} + (1 - \frac{1}{\omega})\phi^{\circ}_{i,j,k} \tag{11}$$

where ω is the over-relaxation factor (Jameson, 1974).

Second derivatives of the potential function ϕ that appear in Eq. (5) are approximated by type-dependent finite-differences. This means that all the second derivatives designated by the superscript E contained in Eq. (5) were approximated by the central differences as follows:

$$(\phi_{,XX})^{E}_{i,j,k} = (\phi^{\circ}_{i+IR,j,k} - 2\phi_{i,j,k} + \phi^{+}_{i-IR,j,k})/(\Delta X)^2$$

with similar expression for $(\phi_{,ZZ})^{E}_{i,j,k}$, while

$$(\phi_{,YY})^{E}_{i,j,k} = (\phi^{+}_{i,j+1,k} - 2\phi^{+}_{i,j,k} + \phi^{+}_{i,j-1,k})/(\Delta Y)^2 \tag{12}$$

and

$$(\phi_{,XY})^{E}_{i,j,k} = (IR)(\phi^{\circ}_{i+IR,j+1,k} - \phi^{+}_{i-IR,j+1,k} - \phi^{\circ}_{i+IR,j-1,k} + \phi^{+}_{i-IR,j-1,k})/(4\Delta X\Delta Y)$$

with similar expressions for $(\phi_{,YZ})^{E}_{i,j,k}$, while

$$(\phi_{,XZ})^{E}_{i,j,k} = (IR)(\phi^{\circ}_{i+IR,j,k+1} - \phi^{\circ}_{i-IR,j,k+1} - \phi^{\circ}_{i+IR,j,k-1} + \phi^{\circ}_{i-IR,j,k-1})/(4\Delta X \Delta Z)$$

where IR = ±1 and JR = ±1 correspond to $U_r \gtrless 0$ and $V_r \gtrless 0$ respectively.

Backward (or retarded) finite difference approximations were used to evaluate the contributions to the correction matrix of all those second derivatives of ϕ (designated with the superscript H) that were involved in determination of the s-directional (or streamline) second derivatives of ϕ in the case of locally hyperbolic regions (see Eq. (3)). The finite difference formulas used are of the following type:

$$(\phi_{,XX})^{H}_{i,j,k} = (2\phi^{+}_{i,j,k} - \phi^{\circ}_{i,j,k} - 2\phi^{+}_{i-IR,j,k} + \phi^{\circ}_{i-2IR,j,k})/(\Delta X)^2$$

with similar expressions for $(\phi_{,YY})^{H}_{i,j,k}$ and $(\phi_{,ZZ})^{H}_{i,j,k}$, while

$$(\phi_{,XY})^{H}_{i,j,k} = \frac{(IR)(JR)}{(\Delta X)(\Delta Y)} (2\phi^{+}_{i,j,k} - \phi^{\circ}_{i,j,k} - \phi^{+}_{i-IR,j,k} - \phi^{+}_{i,j-JR,k} + \phi^{\circ}_{i-IR,j-JR,k}) \qquad (13)$$

with similar expressions for $(\phi_{,XZ})^{H}_{i,j,k}$ and $(\phi_{,YZ})^{H}_{i,j,k}$. Using a local (linear) von Neumann stability criterion, Jameson (1974) showed that in the 2-D case when $M_r > 1$ the value of the over-relaxation factor must be $\omega = 2$. Note

that this corresponds to the requirement of zero damping in the ATDE, i.e., $\varepsilon = 0$ when $M_r > 1$. As pointed out by Jameson (1976) and Caughey (1978) damping is necessary only in the case when $M_r < 1$, because this is the only way to remove the dependence of the solution on the initial guess of the potential field. The recommended value of ω for the case when $M_r < 1$ is between $\omega = 1.6$ and $\omega = 1.9$ where larger values should be used on finer grids. It is easy to show that

$$\phi_{,st} = \frac{2}{1 + \sqrt{1+(\Omega r/q_r)^2}} \left(\frac{1}{Dq_r}\right)\left(U_r\phi_{,Xt} + V_r\phi_{,Yt} + W_r\phi_{,Zt}\right)$$

If it is necessary to introduce an explicit term in $\phi_{,st}$ in order to make the ATDE satisfy Eq. (9) (as in the case when $M_r \doteq 1$) and retain the s-coordinate as the time-like direction, this should serve as a guide-line for the construction of such a term. Also, it can be shown (Dulikravich, 1979) that the finite difference approximation of $(M_r^2-1)\phi^H_{,ss}$ contributes to α_1 the following term:

$$(M_r^2-1)\left(\frac{\Delta t}{Dq_r}\right)\left(\frac{1 + \sqrt{1+(\Omega r/q_r)^2}}{2}\right)\left(\frac{U_r}{\Delta X} + \frac{V_r}{\Delta Y} + \frac{W_r}{\Delta Z}\right)$$

The set of nonhomogeneous, nonlinear, algebraic equations of the general matrix form:

$$[\delta]\{C\} + \{REZ\} = 0$$

was obtained from the discretization of the FPE, where $[\delta]$ is a tri-diagonal coefficient matrix, $\{C\}$ is the vector of the corrections to be subtracted from the values of the potential ϕ at every point on the same mesh line and $\{REZ\}$ is the vector of the residuals of the discretized FPE at every point on the same

mesh line. It was solved semi-iteratively. The elimination method of Crout or Cholesky (Willems and Lucas, 1968) was used to directly invert [δ] for all mesh points situated along the same mesh line. Because ΔX = ΔY = ΔZ = 2 the terms of [δ] and {REZ} that were obtained from Eqs. 5,10,11,12 and 13 can be multiplied through by the factor of 4 and written in the following form:

$$\xi C_{i,j-1,k} + \eta C_{i,j,k} + \zeta C_{i,j+1,k} + REZ_{i,j,k} = 0$$

where the coefficients are (in their most general form)

$$\xi = -S_{YY} + R_{YY}(2+JR) + \left(\frac{1+JR}{2}\right)((IR)(JR)R_{XY} + (JR)R_{YZ})$$

$$\eta = 2\left(S_{YY} + \frac{1}{\omega}(S_{XX}+S_{ZZ})\right) +$$

$$- 2((IR)(JR)R_{XY} + (IR)R_{XZ} + (JR)R_{YZ}) +$$

$$- 4R_{YY} - 2\left(1 + \frac{1}{\omega}\right)(R_{XX}+R_{ZZ})$$

$$\zeta = -S_{YY} + R_{YY}(2-JR) + \left(\frac{1-JR}{2}\right)((IR)(JR)R_{XY} + (JR)R_{YZ})$$

where $\omega = 2$ in the case of locally supersonic relative flow, while the total residual is

$$
\begin{aligned}
REZ_{i,j,k} = {} & 4(a^2(U^E_{r,X}+V^E_{r,Y}+W^E_{r,Z}) - \\
& - (U_r Q^E_{,X}+V_r Q^E_{,Y}+W_r Q^E_{,Z}))_{i,j,k} + \\
& + 4(RVISC)_{i,j,k} + \\
& + C_{i-IR,j,k}(-S_{XX}+3R_{XX}+(IR)(JR)R_{XY} + \\
& + (IR)R_{XZ}) + \\
& + C_{i,j,k-1}(-S_{ZZ}+3R_{ZZ}+(IR)R_{XZ}+(JR)R_{YZ}) + \\
& + \frac{(IR)}{4}(S_{XY}-R_{XY})(C_{i-IR,j+1,k}-C_{i-IR,j-1,k}) + \\
& + \frac{1}{4}(S_{YZ}-R_{YZ})(C_{i,j+1,k-1}-C_{i,j-1,k-1})
\end{aligned}
$$

Because formulas in Eq. (5) result in

$$
(\phi^{\circ H}_{,XX}-\phi^{\circ E}_{,XX})_{i,j,k} = -(IR)\Delta X(\phi^{\circ E}_{,XXX})_{i-IR/2,j,k}
$$

and similar expressions for other differences, one can write the artificial viscosity contribution to the residual to be approximately:

$$
(RVISC) \doteq (f^H_{,X}+g^H_{,Y}+h^H_{,Z})
$$

where:

$$
(f)_{i,j,k} = -\frac{(IR)}{2}[\Delta X(2R_{XX}\phi^{\circ E}_{,XX}+R_{XY}\phi^{\circ E}_{,XY}+R_{XZ}\phi^{\circ E}_{,XZ})]_{i,j,k}
$$

$$
(g)_{i,j,k} = -\frac{(JR)}{2}[\Delta Y(R_{YX}\phi^{\circ E}_{,YX}+2R_{YY}\phi^{\circ E}_{,YY}+R_{YZ}\phi^{\circ E}_{,YZ})]_{i,j,k}
$$

$$
(h)_{i,j,k} = -\frac{(KR)}{2}[\Delta Z(R_{ZX}\phi^{\circ E}_{,ZX}+R_{ZY}\phi^{\circ E}_{,ZY}+2R_{ZZ}\phi^{\circ E}_{,ZZ})]_{i,j,k}
$$

This manipulation enables one to write the modified continuity equation (see Eq. (7)) in the so-called quasi-conservative form (Caughey and Jameson, 1977) as follows:

$$[a^2(U_{r,X}+V_{r,Y}+W_{r,Z})-(U_rQ_{,X}+V_rQ_{,Y}+W_rQ_{,Z})]+(RVISC) = 0$$

where the basic part of the conservation equation has been calculated in nonconservative form, while the artificial viscosity is added in a conservative form.

In the limit as the mesh size goes to zero the artificial viscosity will vanish, but the possible discontinuities in the solution will not, in general, be of exactly the same strength and at the same position as the weak solution of the FPE written entirely in the conservation form (Arlinger, 1975). In certain flow calculations it was shown that this difference is negligible (Bauer and Korn, 1975). Caughey (1979) proved that this is the case only if the shock is weak. Eq. (7) is satisfied numerically within each control space. Such an Auxiliary Control Cell (ACC) is centered around each mesh point (see Fig. (4) for 2-D case) i.e., it is formed of the parts of the eight (in 3-D) Elementary Mesh Cells (EMC) that meet at the same mesh point.

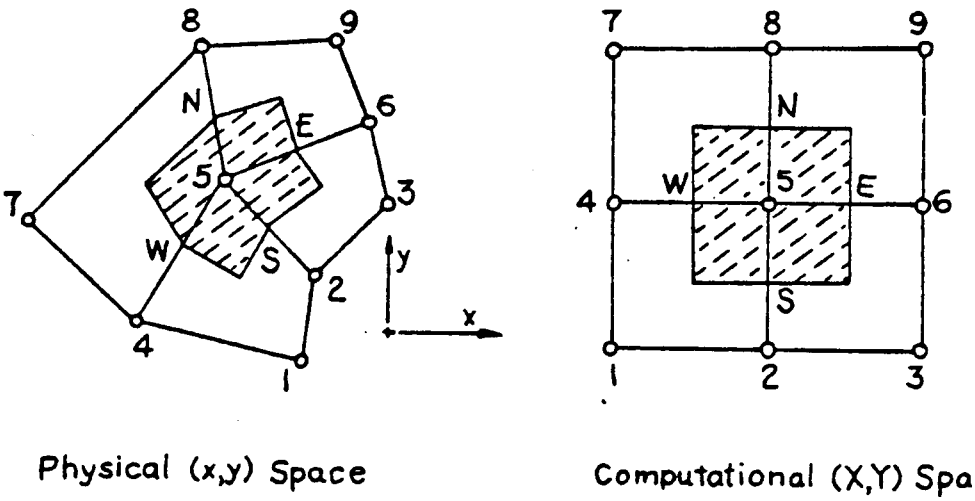

Fig. 4. Auxiliary and Elementary Mesh Cells in the Two-Dimensional Case.

The present numerical scheme was adopted following Caughey (Caughey and Jameson, 1977). It assumes that the sides of an ACC are placed halfway between the two neighboring mesh points in each computational direction and that the derivatives of flow and geometric parameters on each surface of an ACC are equal to their values at the center of the particular surface (i.e., points N,S,W and E shown on Fig. 4. The central point of each surface of an ACC is shared by the four (in 3-D) neighboring EMC. The value of the desired parameter at the center of each face of an ACC was evaluated as an arithmetic mean of the four separate results calculated on the basis of the local mapping functions in each of the four neighboring EMC. As a result, one gets the following general set of finite difference approximations where b stands for $x,y,z,f,g,h,U_r,V_r,W_r,Q,G$ or ϕ.

$$(b_{,X})_{i\pm\frac{1}{2},j,k} = \pm\left(\frac{1}{2}\right)(b_{i\pm1,j,k} - b_{i,j,k})$$

$$(b_{,X})_{i,j\pm\frac{1}{2},k} = \frac{1}{8}\,(b_{i+1,j,k} - b_{i-1,j,k} + b_{i+1,j\pm1,k} -$$

$$- b_{i-1,j\pm1,k})$$

$$(b_{,X})_{i,j,k\pm\frac{1}{2}} = \frac{1}{8}\,(b_{i+1,j,k} - b_{i-1,j,k} + b_{i+1,j,k\pm1} -$$

$$- b_{i-1,j,k\pm1})$$

with analogous formulas for Y and Z differences.

On the solid boundaries, boundary conditions were explicitly applied by incorporating that $V_r = 0$ (or that $V_r = W_r = 0$ in 3-D case) directly in Eq. 6 and Eq. 7 at boundary points.

VI. Results of the Numerical Computations.

On the basis of the previous analysis, two separate computer programs were developed: CAS2D, which numerically solves the FPE for flows through 2-D stationary blade rows and CAS3D which numerically solves the FPE for flows through 3-D stationary or rotating cascades of blades mounted on a doubly infinite cylindrical hub. These 3-D cascades can be isolated or ducted i.e., confined within a doubly infinite cylindrical duct.

VI.1. 2-D Results.

The calculations performed by CAS2D were done on three consecutive meshes consisting of 24 x 6, 48 x 12 and 96 x 24 mesh cells correspondingly. A typical (24 x 6) mesh is shown in Fig. 5. After the circulation converged on each mesh, the values of the reduced potential were interpolated onto the next finer mesh and used as an improved initial guess for the iterative solution on that mesh.

The simplest case for which CAS2D was tested was the nonlifting steady potential flow of an incompressible fluid (taking $M_{-\infty} = 0.001$). A cascade of symmetric NACA 0012 airfoils at zero angle of attack and at zero stagger angle ($\beta=0°$) with a relatively high gap-to-chord ratio ($t/c = 3.6$) was tested and the result was compared with an exact solution (Caughey (1977)) for a NACA 0012 airfoil in free air (Fig. 6). The agreement is excellent, as it is in the case of an incompressible lifting flow (Fig. 7). Here the comparison was made with an exact result of Gostelow (1965).

In order to test the transonic capabilities of the program, a cascade of symmetric NACA 0012 airfoils was tested at zero angle of attack ($\alpha_{-\infty} = 0°$), zero stagger angle ($\beta = 0°$), gap-to-chord ratio $t/c = 3.6$ and $M_{-\infty} = 0.8$. Results (Fig. 8) agree very well with the calculations of Caughey (1979a) for the identical case.

The final test was for a transonic lifting case. Because of unavailability of published test cases appropriate for the analysis using CAS2, we analyzed a shockless cascade designed by Jose Sanz (1979) who used the Garabedian-Korn hodograph technique. The open trailing edge of the original profile was rounded and effect of the wake thickness was taken into account via a quasi-three-dimensional flow assumptions. The agreement of the CAS2D result (Fig. 9) with that of Sanz is very good (Dulikravich, 1980), especially if one considers geometric modifications that were performed.

Results of 3-D Computer Program.

CAS3D was developed with CAS2D serving as a guideline.

The test case was chosen to be a rotor in a cylindrical doubly infinite duct. The rotor consisted of 8 blades that had no taper, no sweep or dihedral. The local airfoil shape was NACA 0012 and the ratio of hub-to-tip radii was 0.85. The twist (stagger) angle of -4° was kept constant along the blade. Chord length normalized by the tip radius was $c/r_t = 0.1$. The axial Mach

number at upstream infinity was $(M_{axial})_{-\infty} = 0.7065$ while the relative tip Mach number was $(M_r^{tip})_{-\infty} = 0.750$. The rotor rotated at $\Omega = 120$ r.p.m. The calculation was performed first on 24 x6 x 3 mesh. The values of the potential after 167 iterations were interpolated on a 48 x 12 x 6 mesh and an additional 55 iterations were performed. The results are shown in Fig. 10. Shock strengths and positions are not very satisfactory because of the coarse mesh and the small number of iterations used.

Conclusion

The assumptions and restrictions pertaining to the full potential flow through 2-D and 3-D cascades were reviewed. Periodicity and boundary conditions were derived together with a canonical form of the full potential equation. A body conforming grid generation for cascades of airfoils based on conformal mapping was developed.

A numerical procedure in the computational space formed by the use of linear isoparametric local mapping functions was detailed together with the way that residuals were calculated and an artificial viscosity introduced. Computer programs were developed and tested using the above analysis. They were proven to be fast, stable and reliable for both lifting and non-lifting, subsonic and transonic flow calculations.

Acknowledgement

The authors are grateful to the Office of Naval Research for support under Contract N00014-77-C-0033, and to the National Research Council and the Computational Fluid Mechanics Branch of NASA Lewis Research Center for additional support.

BIBLIOGRAPHY

1. Arlinger, G.B., "Axisymmetric Inlet Flow at Low Supersonic Mach Numbers", Symposium Transsonicum II, Springer-Verlag, Gottingen, 1975.

2. Bauer, F., and Korn, D., "Computer Simulation of Transonic Flow Past Airfoils with Boundary Layer Correction", Proceedings of the AIAA 2nd Computational Fluid Dynamics Conference, Hartford, Connecticut, June 19-20, 1975, pp. 200.

3. Carrier, F.G., and Pearson, R.C., Partial Differential Equations, Academic Press, 1976, pp. 230.

4. Caughey, D.A., and Jameson, A., "Numerical Calculation of Transonic Potential Flow About Wing-Fuselage Combinations", AIAA Paper 77-677, 1977 (also AIAA Journal, Vol. 17, pp. 175-181, Feb. 1979).

5. Caughey, D.A , private communication, 1977.

6 Caughey, D.A., "Numerical Calculation of Transonic Potential Flows", Lectures presented at a Short Course on Advances in Computational Fluid Dynamics at the University of Tennessee Space Institute, Tullahoma, Tennessee, December 4-8, 1978.

7. Caughey, D.A. and Jameson, A., "Recent Progress in Finite-Volume Calculations for Wing-Fuselage Combinations", AIAA Paper 79-1513, presented at AIAA 12th Fluid and Plasmadynamics Conference, Williamsburg, July 23-26, 1979.

8. Caughey, D.A., private communications, 1979a.

9. Dulikravich, D S., "Numerical Calculation of Inviscid, Potential Transonic Flows Through Rotors and Fans", Ph.D. Thesis, Cornell University, January 1979.

10. Dulikravich, D.S., "CAS2D: Computer Program for Planar Steady Potential Transonic Cascade Flows", to be published as NASA TP, 1980.

11. Foley, M.W., "From daVinci to the Present - A Review of Airscrew Theory for Helicopters, Propellers, Windmills and Engines", AIAA Paper No. 76-367, 9th Fluid and Plasma Dynamics Conference, San Diego, July 14-16 1976.

12. Garabedian, P., "Estimation of the Relaxation Factor for Small Mesh Sizes", Math. Tables and Aids to Comput., Vol. 10, 1956, pp. 183-185.

13. Garrick, I.E., "On the Plane Potential Flow Past a Lattice of Arbitrary Airfoils", NACA Report No. 788, 1944.

14. Gostelow, J.P., "Potential Flow Through Cascades - A Comparison Between Exact and Approximate Solutions", A.R.C. C.P. No. 807, 1965.

15. Hayes, W.D., Gasdynamic Discontinuities, No. 3, Princeton Aeronautical Paperbacks, Princeton University Press, 1960.

16. Ives, D. and Liutermoza, Jr., "Analysis of Transonic Cascade Flow Using Conformal Mapping and Relaxation Techniques", AIAA Paper No. 76-370, AIAA 9th Fluid and Plasma Dynamics Conference, San Diego, July 14-16, 1976.

17. Jameson, A., "Iterative Solution of Transonic Flows Over Airfoils and Wings, Including Flows at Mach 1", Commun. Pure & Appl. Math., No. 27, pp. 283-309, 1974.

18. Jameson, A., "Transonic Flow Calculations", Lectures Presented at Von Karman Institute, March 11-15, 1976.

19. Jameson, A. and Caughey, D., "A Finite Volume Scheme for Transonic Potential Flow Calculations", Proceedings of AIAA 3rd Computational Fluid Dynamics Conference, Albuquerque, New Mexico, June 27-28, 1977.

20. Kaiho, T., "A New Method for Solving Surface-Piercing-Strut Problems", Department of Naval Architecture and Marine Eng., The University of Michigan, Ann Arbor, Report No. 196, 1978.

21. Kober, H., Dictionary of Conformal Representations, Dover Publications, Inc., 1957, pp. 131.

22. Okurounmu, O. and McCune, J.E., "Three-Dimensional Vortex Theory of Axial Compressor Blade Rows at Subsonic and Transonic Speeds", AIAA Journal, Vol. 8, No. 7, July 1970.

23. Rae, J.W., "Nonlinear Small-Disturbance Equations for Three-Dimensional Transonic Flow Through a Compressor Blade Row", Calspan Report No. AB-5487-A-1, August 1976.

24. Robinson, A. and Laurman, J.A., Wing Theory, Cambridge at the University Press, 1956, pp. 75-79.

25. Jose Sanz, NASA Langley, ICASE (private communications),October 1979.

26. Spiegel, M.R., Mathematical Handbook, Schaum's Outline Series, McGraw-Hill Book Company, 1968.

27. Steger, J.L. and Baldwin, B.S., "Shock Waves and Drag in the Numerical Calculations of Isentropic Transonic Flow", NASA TN-6997, October 1972.

28. Theodorsen, T., "Theory of Wing Sections of Arbitrary Shape", NACA Report No. 411, 1931.

29. Vavra, M.H., Aero-Thermodynamics and Flow in Turbomachines, John Wiley & Sons, Inc., 1960, pp. 122-125.

30. Willems, N. and Lucas, W., Matrix Analysis for Structural Engineers, Prentice-Hall, 1968, pp. 46-50.

31. Von Mises, Mathematical Theory of Compressible Fluid Flow, edited by Ludford, G.S.S., Academic Press, New York, 1958, pp. 112-114.

32. Wu, Chung-Hua, "A General Theory of Three-Dimensional Flow in Subsonic and Supersonic Turbomachines of Axial-, Radial-, and Mixed-Flow Types", NACA TN 2604, January 1952.

FIGURE CAPTIONS

Figure 5. Typical mesh for cascade calculation (coarse mesh consisting of 24 x 6 cells).

Figure 6. Incompressible solutions for NACA 0012 airfoil in solid-walled tunnel. $M_\infty = 0.001$, $t/c = 3.6$; o current results; —— exact solution for free-air case.

Figure 7. Incompressible flow past lifting cascade. o current results; —— Gostelow (1965).

Figure 8. Transonic flow past NACA 0012 airfoil in solid-walled tunnel. $M_\infty = 0.8$, $t/c = 3.6$; o current results; —— Caughey (1979a).

Figure 9. Transonic flow past shockless-design cascade. o current results —— Sanz (1979).

Figure 10. Transonic flow past lifting rotor. $(M_{axial})_\infty = 0.7458$, $(V/nD) = .082$. o suction side; Δ pressure side.

(a) $r/r_{tip} = 0.85$
(b) $r/r_{tip} = 1.00$

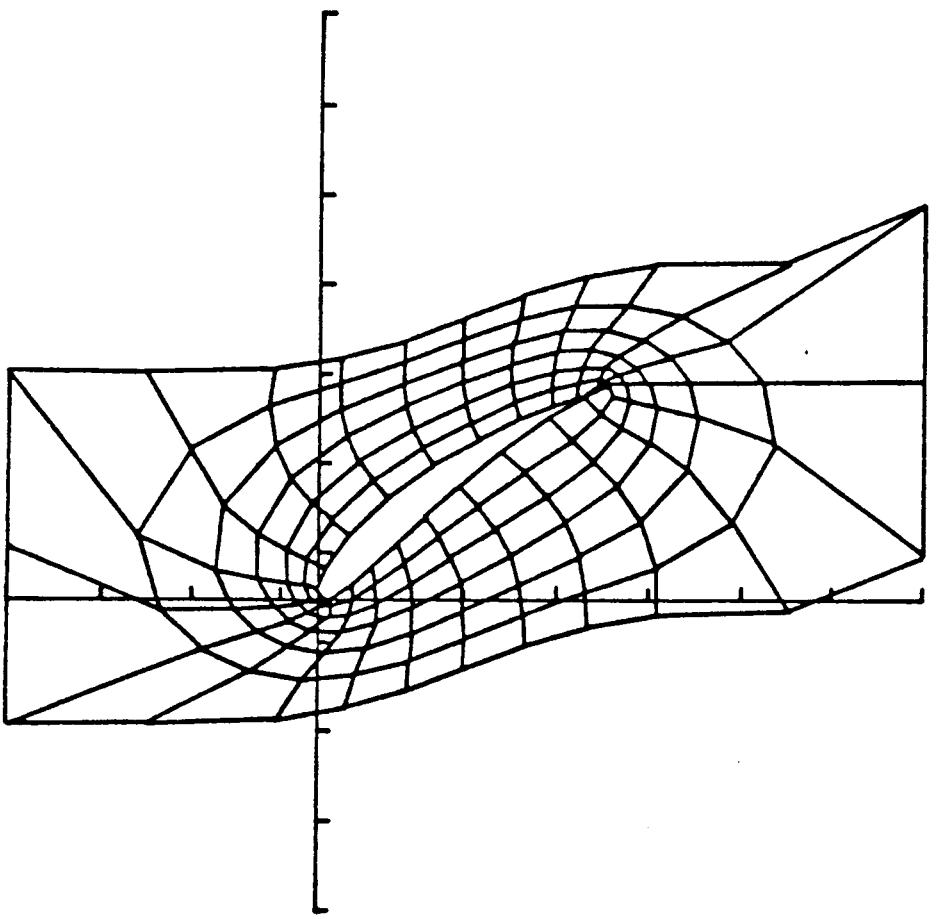

Figure 5

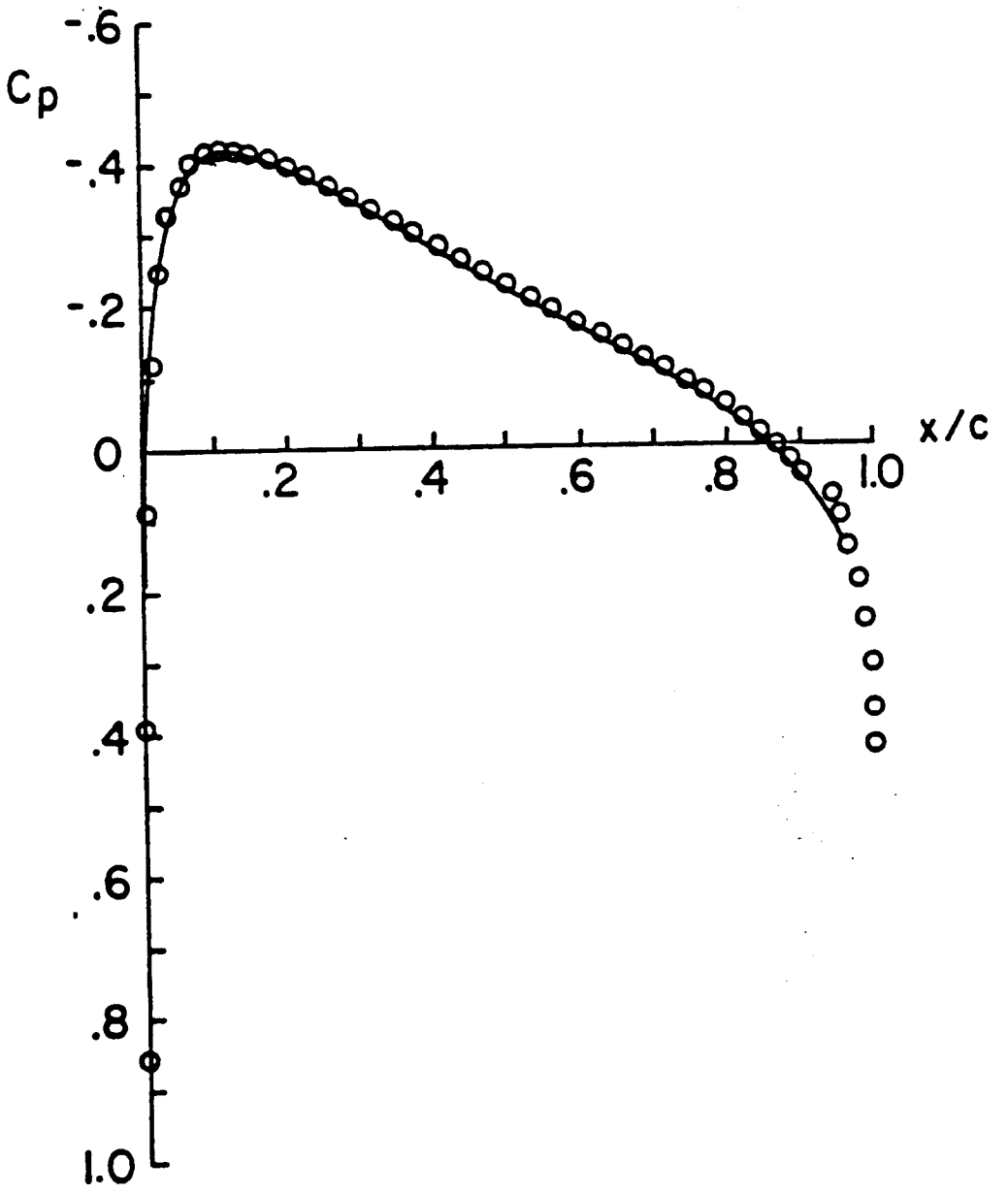

Figure 6

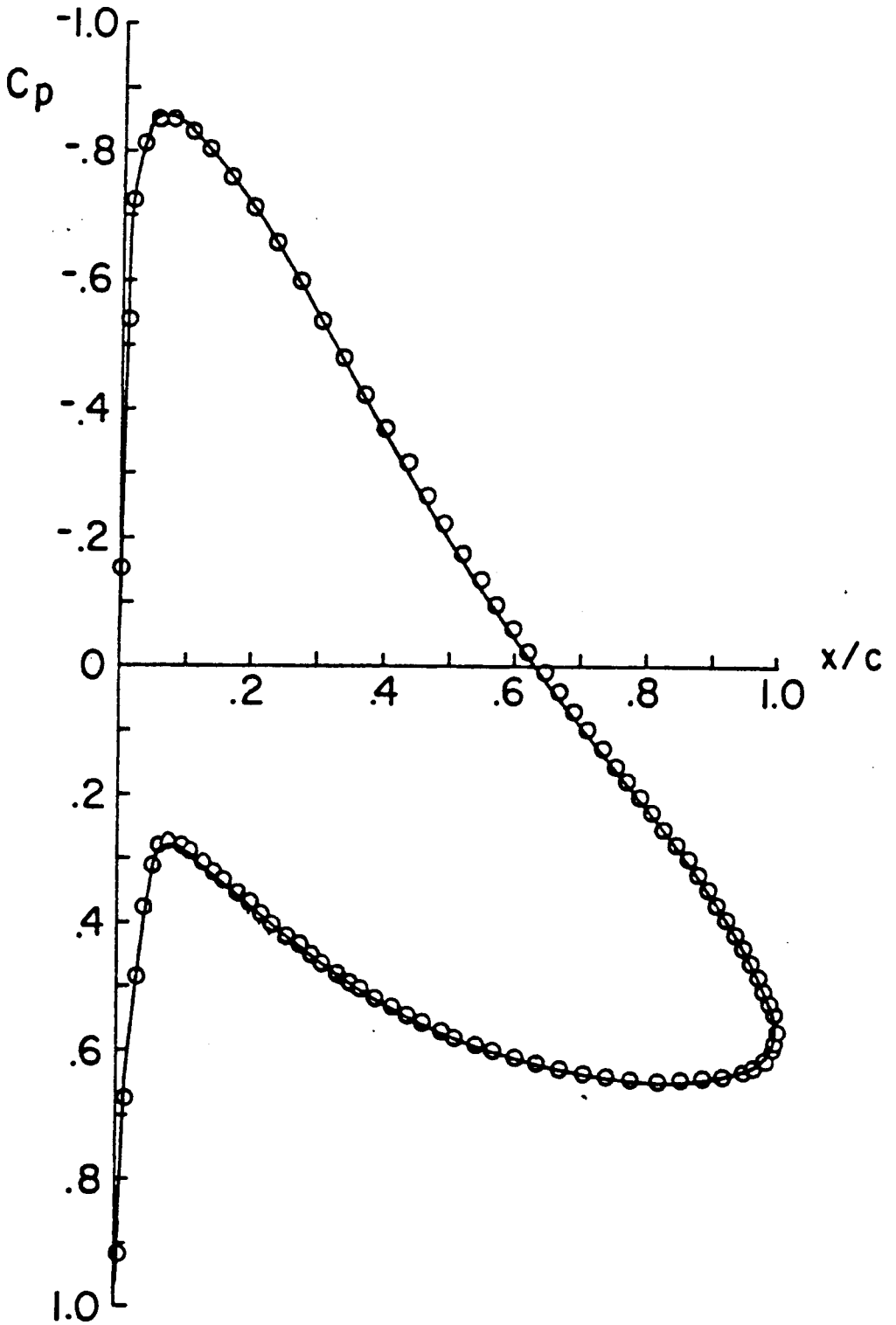

Figure 7

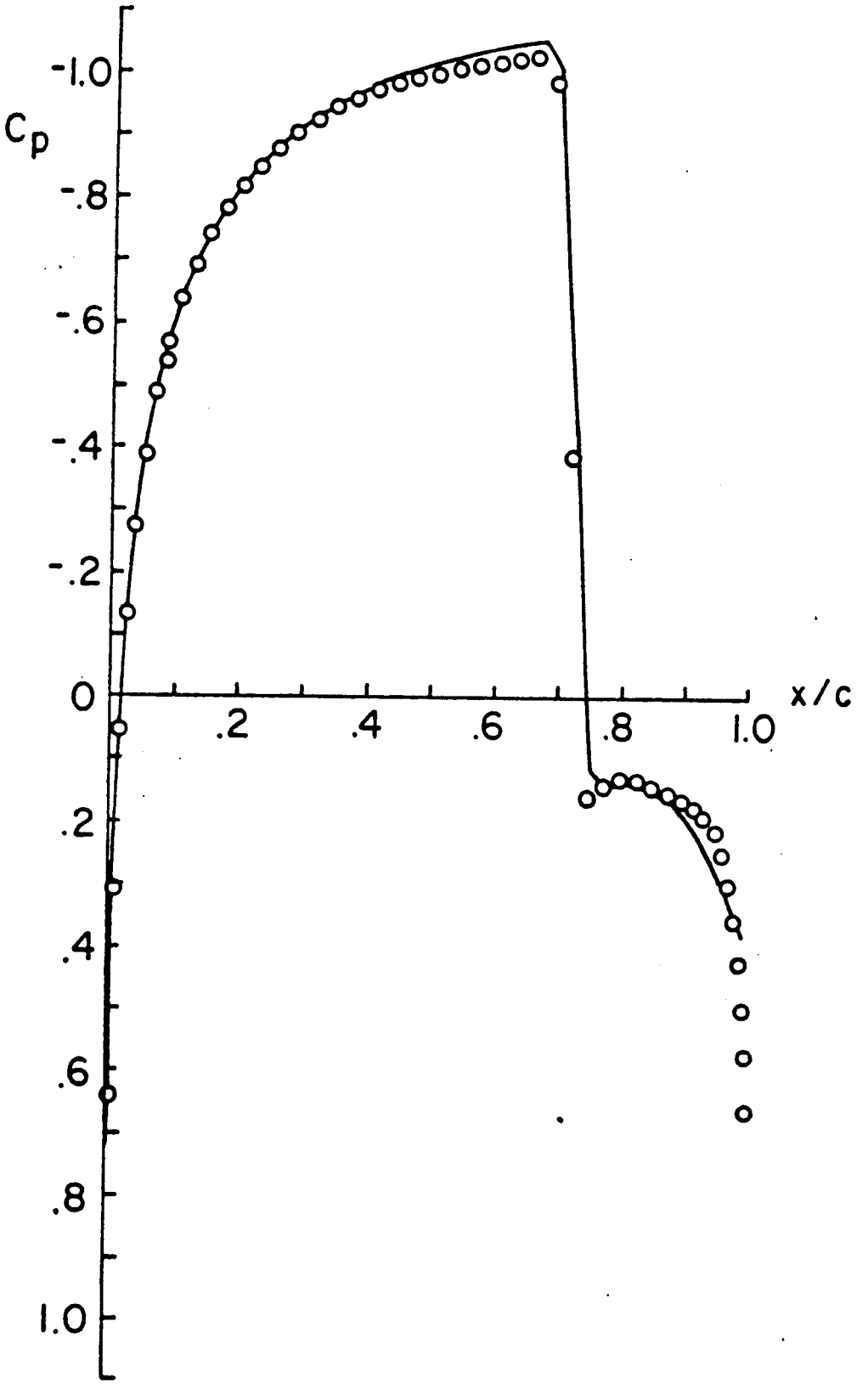

Figure 8

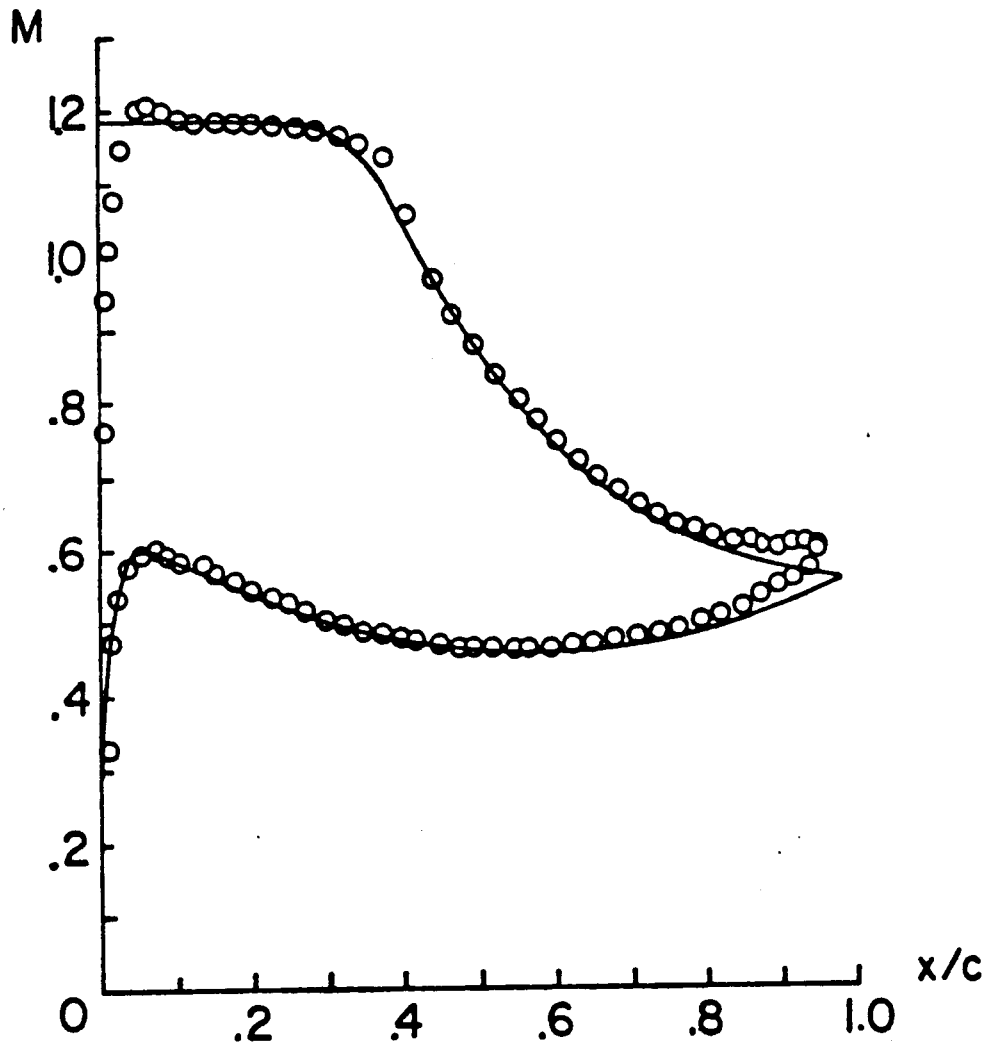

Figure 9

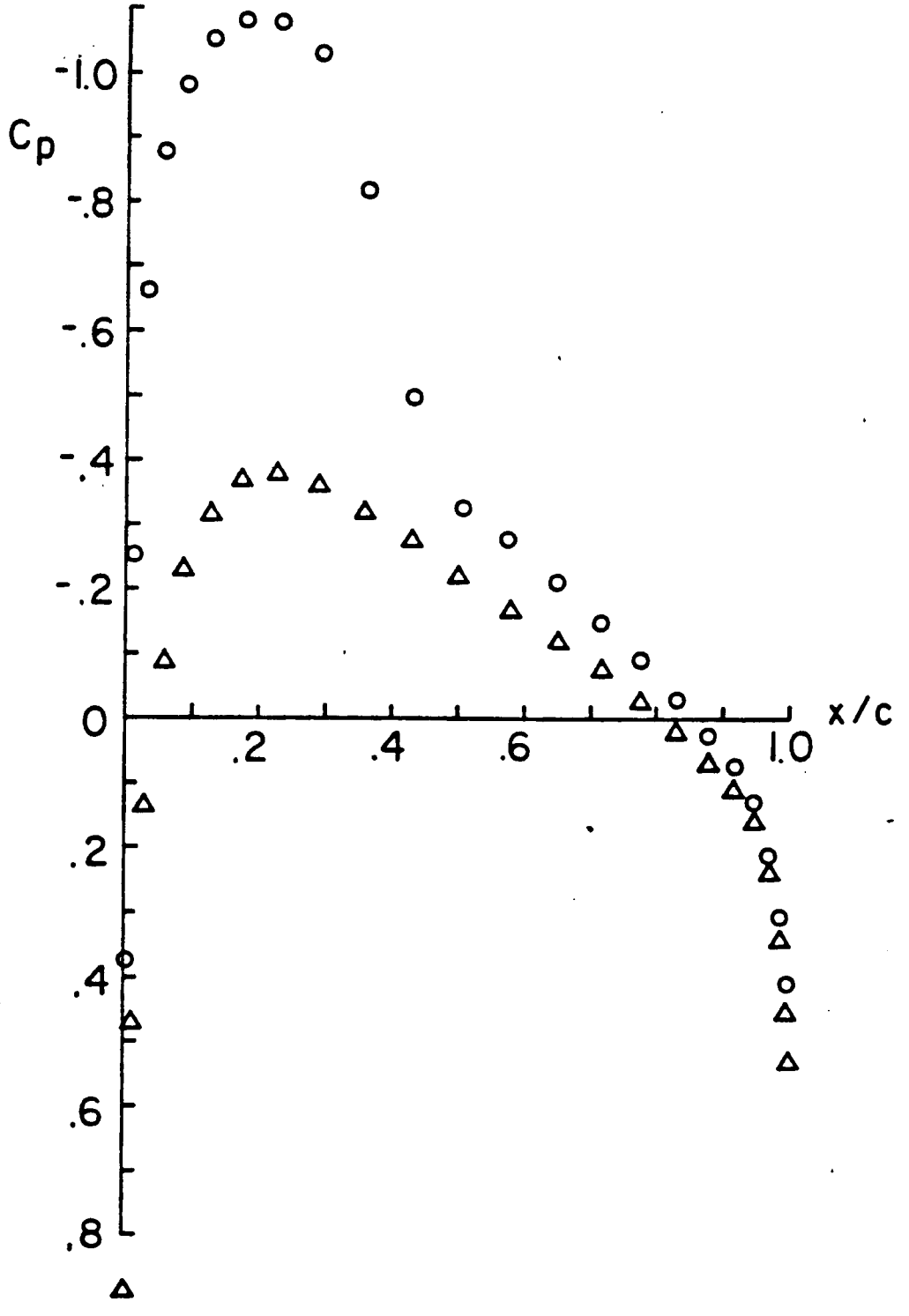

Figure 10a

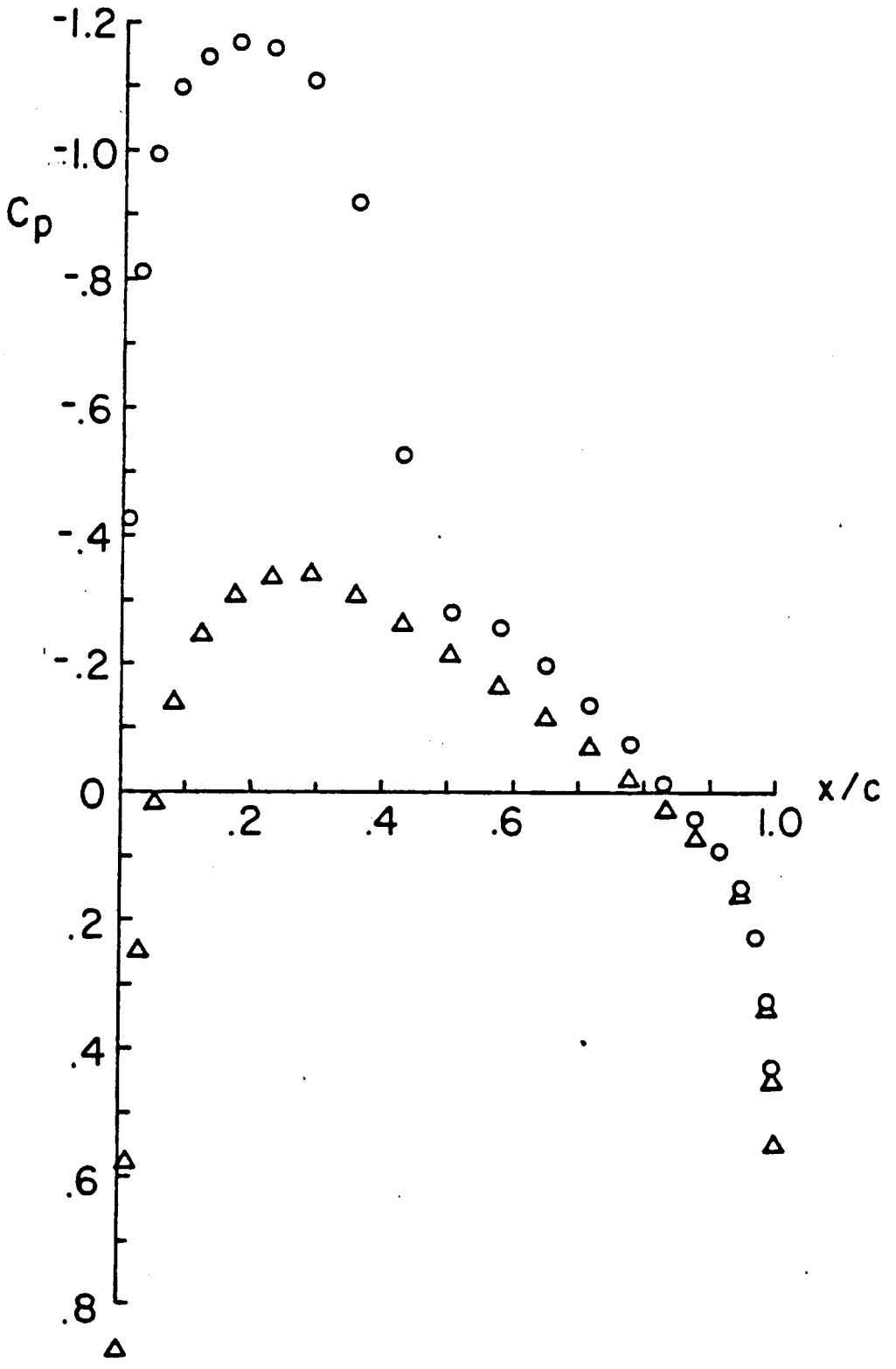

Figure 10b